Formation of vs. Recruitment to RNA-Rich Condensates: Controlling Effects Exerted by Peptide Side Chain Identity

Jiani Niu,[1] Cindy Qiu,[2] Nicholas L. Abbott,[2,*] Samuel H. Gellman[1,*]

[1]Department of Chemistry, University of Wisconsin-Madison, Madison, Wisconsin 53706, USA.

[2]Robert F. Smith School of Chemical and Biomolecular Engineering, Cornell University, New York 14853, USA

ABSTRACT: Liquid-liquid phase separation (LLPS), which is the spontaneous formation of contiguous liquid phases with distinct compositions, has been long known in chemical systems and more recently recognized as a ubiquitous feature of cell biology. We describe an LLPS system involving biologically relevant components, synthetic peptides and total yeast RNA, that has enabled us to explore factors that underlie phase separation. We find that Coulombic complementarity between a cationic peptide and anionic RNA is necessary but not sufficient for LLPS in our system. In addition to a net positive charge, the peptide must present the proper type of cationic moiety. Guanidinium groups, as found in the Arg side chain, support LLPS, but ammonium groups, as found in the Lys side chain, or dimethylguanidinium groups, as found in post-translationally modified Arg side chains, do not support LLPS. We further show that cationic groups not competent to support formation of a condensed phase via interaction with RNA can nevertheless enable recruitment to a condensed phase, which reveals that the network of forces governing condensed phase formation can differ from the network of forces governing recruitment to such a phase. We introduce a new method for measuring the concentrations of components in condensed phases based on fluorine-containing additives and ^{19}F NMR.

INTRODUCTION

Liquid-liquid phase separation (LLPS) mediated by biopolymers generates membraneless organelles and other types of condensates that are important features of the dynamic internal environment in cells.[1–3] New participants in condensate formation and new physiological roles for LLPS are being uncovered at a rapid pace. Biomolecule-based phase separation phenomena can be roughly divided into two classes.[4] One type of LLPS (designated *class I* here) relies on multivalent protein-protein or protein-nucleic acids interactions involving well-folded and specific recognition modules that are linked by flexible and often disordered segments.[5–11] The other type (designated *class II* here) is mediated by small molecular features, such as individual protein side chains, that are dispersed within biopolymer components.[12–15] Proteins or protein domains that support *class II* LLPS are typically disordered.[12]

The network of intermolecular forces that results in *class II* phase separation is not always clear. Such systems provide opportunities to discover new principles of molecular assembly that underlie formation of condensed phases, including but not limited to principles that have been harnessed by evolution. For example, LLPS resulting from interactions of polyanions and polycations is strongly influenced not only by net charge on the individual components but also by the distribution of charged groups along the polymer chains.[16] The stereochemistry of peptide-based polycations or polyanions can affect the physical properties of their assemblies, with heterochiral peptides favoring liquid assemblies relative to homochiral peptides.[17] The nature of charge-bearing groups can modulate the physical properties of condensed phases formed by polycation-polyanion pairing, as illustrated by variations between lysine-based and arginine-based polypeptides (ammonium vs. guanidinium).[18,19]

The biological roles of LLPS are not fully understood,[20,21] but some functions are coming into focus. For example, P-bodies promote RNA processing in the cytoplasm by concentrating the necessary enzymes and their substrates, and the nucleolus is important for ribosome assembly.[22] In addition, membraneless organelles appear to provide spatiotemporal control of cellular signaling.[23] Such functions require that specific biomolecules be recruited to condensed phases within cells. Here we ask whether the molecular features necessary for *formation* of a biopolymer-rich phase via *class II* LLPS can be distinguished from features that allow *recruitment* to a biopolymer-rich phase.

RESULTS

Arginine-rich peptides derived from FUS mediate LLPS in combination with RNA. As a prelude to addressing the formation vs. recruitment question, we sought to identify a biomimetic *class II* LLPS system in which a polypeptide component could be accessed by chemical synthesis. This goal was motivated by our desire to transcend the limits on amino acid composition that are imposed by ribosomal synthesis. Our exploratory efforts were based on Fused in Sarcoma (FUS), an RNA-binding protein that mediates LLPS *in vivo* and that has been extensively studied *in vitro*.[12,24–27] The FUS C-terminal domain (CTD; Figure **1a**) contains three Arg/Gly-rich (RGG) motifs; similar segments occur in other RNA-binding proteins that support membraneless organelle formation.[28] Evaluation of CTD fragments of varying lengths led us to **1**, a 27-mer derived from

FUS (471-497) (Figure **1b**, **S1**) that supports robust LLPS when combined with RNA.

Peptide **1** contains eight native Arg residues. However, **1** differs from the corresponding FUS segment in that the three natural Asp residues were replaced by Glu, to avoid aspartimide formation during peptide synthesis. Peptide **1** should have a net charge of +5 near neutral pH. LLPS could be induced by combining **1** with total yeast RNA. Use of this highly heterogeneous RNA source was expected to minimize the possibility that formation of a condensed phase would be driven by specific RNA-peptide recognition.[18,29]

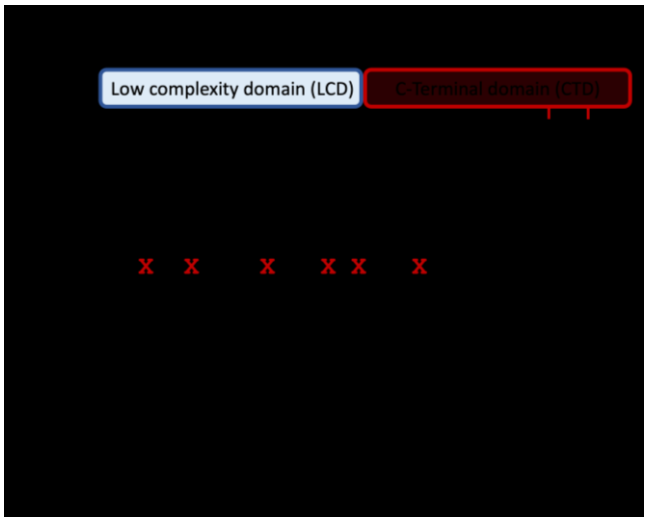

Figure 1. (**a**) Schematic of the protein FUS (1-526). LCD, low complexity domain; CTD, C-terminal domain. Peptides used in this study were derived from FUS (471-497) within the Arg/Gly-rich CTD. (**b**) Primary sequences of FUS (471-497)-derived peptides **1** - **5**. Substitutions are highlighted in red with corresponding amino acids listed on the bottom.

Formation of droplets was observed via microscopy when 0.025-0.1 mM **1** in Tris buffer, pH 7.5, was mixed with 0.25 μg/μL total yeast RNA (referred to as "RNA" below; ~0.8 mM on a per-nucleotide basis). To enable fluorescence microscopy, we included 4 mol% of a derivative of **1** bearing a fluorescein moiety (**Fl-1**, Figure **S2**). Liquid droplets could be observed via differential interference contrast (DIC), fluorescence and Z-stack modes (Figure **2a**, **S3a**). We probed the nature of the droplets by monitoring fluorescence recovery after photobleaching (FRAP; Figure **2b**). A very rapid return to uniform fluorescence was observed after focused irradiation (within ~0.3 s), which indicates that the droplets represent a highly dynamic liquid state.[20]

An increase in average droplet size 30 min after mixing **1**+RNA was observed when the peptide concentration was increased from 0.025 mM to 0.1 mM while holding RNA concentration constant. (Droplet size varies as a function of time, because droplets slowly fuse with one another.) This trend was evident from micrographs (Figure 2a) and confirmed via particle size measurements determined by dynamic light scattering (Figure **S3b**). A concomitant concentration-dependent increase in turbidity was observed over this peptide concentration range (Figure **S3c**).

To test the hypothesis that the condensed phase formed by combining peptide **1** and RNA corresponds to *class II* LLPS, i.e., phase separation mediated by small motifs such as side chains rather than interaction of **1** with a specific, folded RNA partner (e.g., a G-quadruplex[29]), we evaluated the enantiomer of **1** (*ent*-**1**) and a "scrambled" sequence isomer of **1** (*mix*-**1**) (Figure **S4**). For *mix*-**1**, we changed the RGG local sequence motifs to GGR without disturbing the overall charge distribution, which can be important for phase separation.[16] Formation of droplets was observed when either of these peptides was combined with RNA (Figure **S4**). These results suggest that the interactions between RNA and **1**, *ent*-**1** or *mix*-**1** that result in LLPS do not require any particular configuration (i.e., L vs. D) or local sequence (e.g., RGG) within the peptide. Instead, LLPS seems to result from transient noncovalent interactions that involve individual side chains or other small fragments, as expected for *class II* LLPS. Analysis of droplet size by microscopy, however, indicates a statistically different distribution of droplet sizes between the LLPS samples formed after 30 min by **1**+RNA vs. *ent*-**1**+RNA (Figure S4).

Liquid-liquid phase separation caused by mixing of polycations with polyanions, such Arg- or Lys-rich polypeptides and RNA, is well-known.[14,19,30,31] Complex coacervation by polyions with complementary charges has been attributed partially or entirely to Coulombic attractions.[30–32] Polycation-polyanion association leads to entropically favorable release of counterions that were localized around each polyion.[33–35] A role for polycation-polyanion attraction in the LLPS behavior of **1**+RNA is suggested by the observation that addition of ≥500 mM NaCl diminishes the turbidity measured for 0.1 mM **1** + 0.5 μg/μL RNA in pH 7.5 buffer (Figure **S5**). This behavior presumably reflects the screening of polycation-polyanion association by sodium and/or chloride ions.

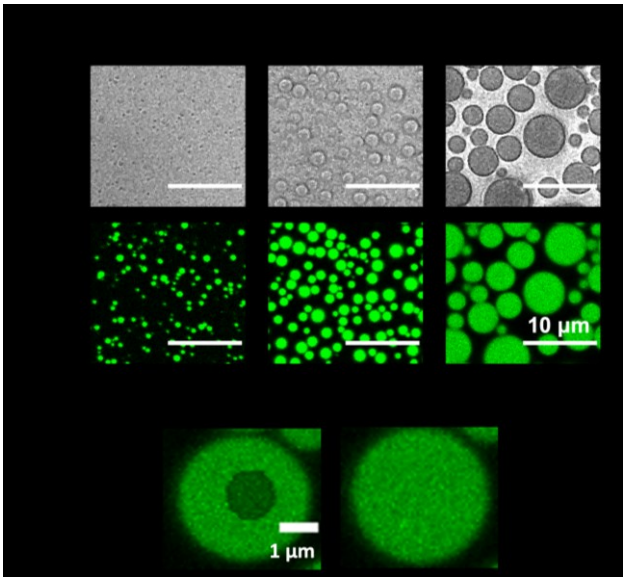

Figure 2. Arg-rich peptide **1** undergoes LLPS when mixed with 0.25 μg/μL total yeast RNA in pH 7.5 buffer. (**a**) Top: liquid droplets of RNA and **1** at different peptide concentrations viewed via differential interference contrast (DIC). Bottom: corresponding fluorescence images in the 488 nm channel (fluorescein, Fl), false colored to green. Scale bar = 10 μm. (**b**) FRAP experiment. Left: A region within a droplet is photobleached (dark; diameter = 1 μm) at T = 0; right: near 100% fluorescence recovery is observed instantly (right, at T = 0.33 sec). Scale bar = 1 μm.

Peptide Side Chain Identity is Critical for Formation of a Condensed Phase. Peptide **2**, an analogue of **1** in which six of the eight Arg residues are replaced with Lys, did not support phase separation under the conditions described above. Specifically, mixing 0.1 mM Lys-rich **2** with 0.25 μg/μL RNA in pH 7.5 buffer did not induce phase separation (Figure **3**), even though Arg-rich **1** and Lys-rich **2** are expected to have a similar net charge in this buffer. Thus, the different behaviors of **1** and **2** suggest that Coulombic attractions cannot fully explain phase separation in solutions of **1**+RNA. Arg vs. Lys differences in LLPS involving proteins or synthetic polypeptides have been previously noted,[12,18,19,30,36] although explanations for these observations have varied, and not all systems display such differences.[25]

Peptides **3**-**5** (Figure **1b**) are analogues of **1** that contain common post-translational modifications at six of the eight Arg positions; this peptide set allowed us to evaluate the impact of each modification on LLPS behavior. Formation of monomethyl-arginine (MMA; peptide **3**), asymmetric dimethyl-arginine (ADMA; peptide **4**) and citrulline (Cit; peptide **5**) are common enzymatic post-translational modifications of arginine *in vivo*.[37,38] MMA and ADMA retain the positive charge of Arg near neutral pH, but Cit is uncharged. We initially probed for LLPS by monitoring light scattering at 600 and 340 nm (Figure **3** and **S6**) when each peptide (0.1 mM) was mixed with 0.25 μg/μL RNA in Tris buffer. MMA-rich peptide **3** caused a modest increase (~60%) in OD_{600} relative to unmethylated peptide **1.** In contrast, no phase separation was observed for ADMA-rich peptide **4** or Cit-rich peptide **5**. The observations with **4** are consistent with reports that the ADMA post-translational modification impairs the ability of FUS to mediate phase separation.[25] The behavior of **5** is consistent with the hypothesis that LLPS upon mixing **1** and RNA is driven at least in part by Coulombic attraction and requires a net positive charge on the peptide. The lack of LLPS observed with asymmetric dimethylated Arg (**1** → **4**), however, supports our conclusion that LLPS induced by mixing **1** and RNA cannot be fully explained by Coulombic interactions.

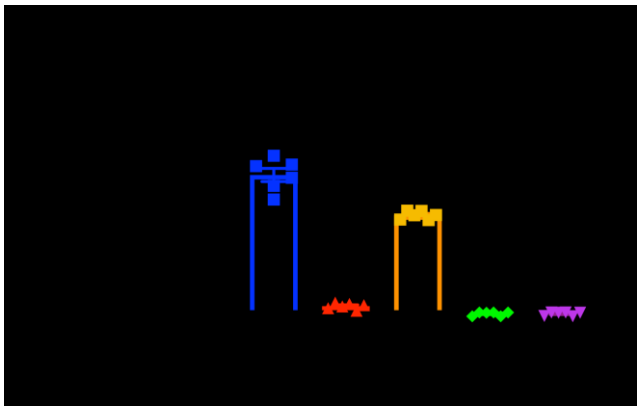

Figure 3. Detection of phase separation for different peptides (0.1 mM) mixed with 0.25 μg/μL RNA by turbidity measurements. Only peptides containing L-Arg, d-Arg or MMA (**1**, *ent*-**1**, and **3**) showed significant turbidity when incubated with RNA in 50 mM Tris, pH 7.5. Data presented as means ± SD (n = 6). P values were calculated by one way ANOVA.

The Ability to Form a Condensed Phase and the Ability to be Recruited to a Condensed Phase Are Distinct Properties. Our observation that the nature of the cationic side chain group determines whether phase separation occurs in the peptide-RNA mixtures described above allowed us to ask whether there is a distinction between the ability to support formation of a biopolymer-rich phase and the ability to be recruited to such a phase. This question was first addressed qualitatively by mixing RNA (final concentration 0.25 μg/μL) with two peptide samples (Figure **4**). Peptide **1** (0.1 mM; containing 4 mol% **Fl-1**) was a component of each mixture to ensure formation of a condensed phase. The second peptide (0.1 mM) was varied but in each case contained 4 mol% of the derivative bearing a tetramethylrhodamine (TMR) label. Fluorescence microscopy allowed independent monitoring of the presence of the two peptides within droplets. As expected, when the second peptide was **1** or *ent*-**1**, the Fl and TMR fluorescence signals co-localized in the droplets (Figure **4a**, **b**).

To our surprise, Lys-rich **2** and ADMA-rich **4** were each concentrated in droplets formed by the interaction of Arg-rich **1** and RNA (Figure **4c**, **d**). In contrast, Cit-rich **5** was not concentrated in the droplets (Figure **4e**). Selective recruitment of the cationic peptides (**1**, **2** and **4**) but not Cit-rich **5** was observed also at lower peptide concentrations (0.025 or 0.05 mM; Figure S7). Z-stack images established that the droplets remained homogeneous (Figure **S8**), i.e., that the Fl and TMR signals were evenly distributed within the droplets. Overall, these results indicate that the Lys-rich peptide **2** and the ADMA-rich peptide **4** can be recruited to an RNA-rich condensed phase, even though neither **2** nor **4** independently supports phase-separation with RNA under these conditions (Figure **3**).

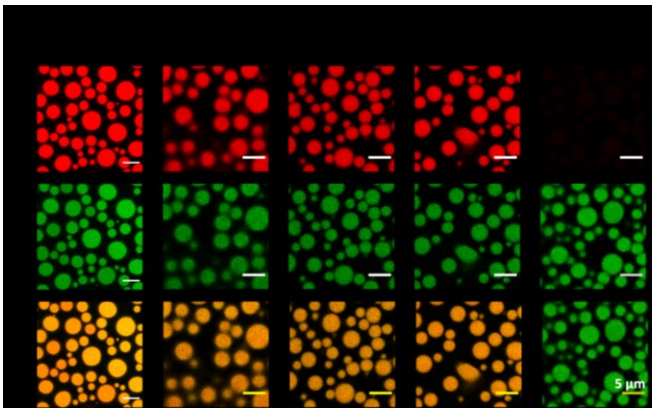

Figure 4. Selective recruitment of peptides to RNA-rich droplets. (**a-d**) Colocalization of various of peptides (**1**, *ent*-**1**, **2**, or **4** containing 4 mol% TMR-labeled derivative) with peptide **1** (containing 4 mol% Fl-labeled derivative) in the condensed phase with RNA. (**e**) Cit-rich peptide **5** was not detected in the droplets. 0.1 mM of each peptide and 0.25 μg/μL RNA were incubated at room temperature for 30 min before images were taken. Scale bar = 5 μm.

To gain further insight on formation of and recruitment to condensed phases described above, we sought to quantify the components within these phases (Figure **S9a**). Measuring concentrations of components within liquid droplets is challenging. Strategies based on fluorescence microscopy require complex analysis and careful controls.[13,39,40] We developed a new and simple method to assess peptide concentrations in the RNA-rich condensed phases described here.

Direct measurement of condensed phase volume is difficult or impossible at the experimental scales typical for these studies, which hampers determination of component concentrations.[13] We reasoned that including a fluorine-containing compound that has no preference between the phases resulting from LLPS, i.e., a species that is neither concentrated in nor excluded from the condensed phase, would allow us to determine the volume of the condensed phase based on ^{19}F NMR measurements (Figure **S9b**). LLPS was induced by combining 0.1 mM **1** and 0.25 μg/μL RNA in 0.6 mL of 50 mM Tris, pH 7.5, with 5 mM of a fluorine-containing additive (identified below). After 30 min, centrifugation was used to isolate the condensed phase, which was then dissolved in 0.6 mL of 0.5 M aqueous NaCl (Figure **S9c**). At this stage, the concentration of the fluorine-containing compound could be determined via integration of the ^{19}F NMR signal, based on an externally generated calibration curve. To test the assumption that the fluorine-containing additive had no phase preference, we conducted parallel studies with two simple salts (NaF and $NaBF_4$) and three small molecules (N-trifluoroacetyl-D-glucosamine, trifluoroacetyl glycine, and trifluoroacetamide). All five provided similar estimates of condensed phase volume, ~1% of the total LLPS solution (Table **S1**). Because physical properties vary among these five fluorine-containing compounds, the similar outcomes support our hypothesis that these fluorine-containing compounds are neither concentrated in nor excluded from the condensed phase.

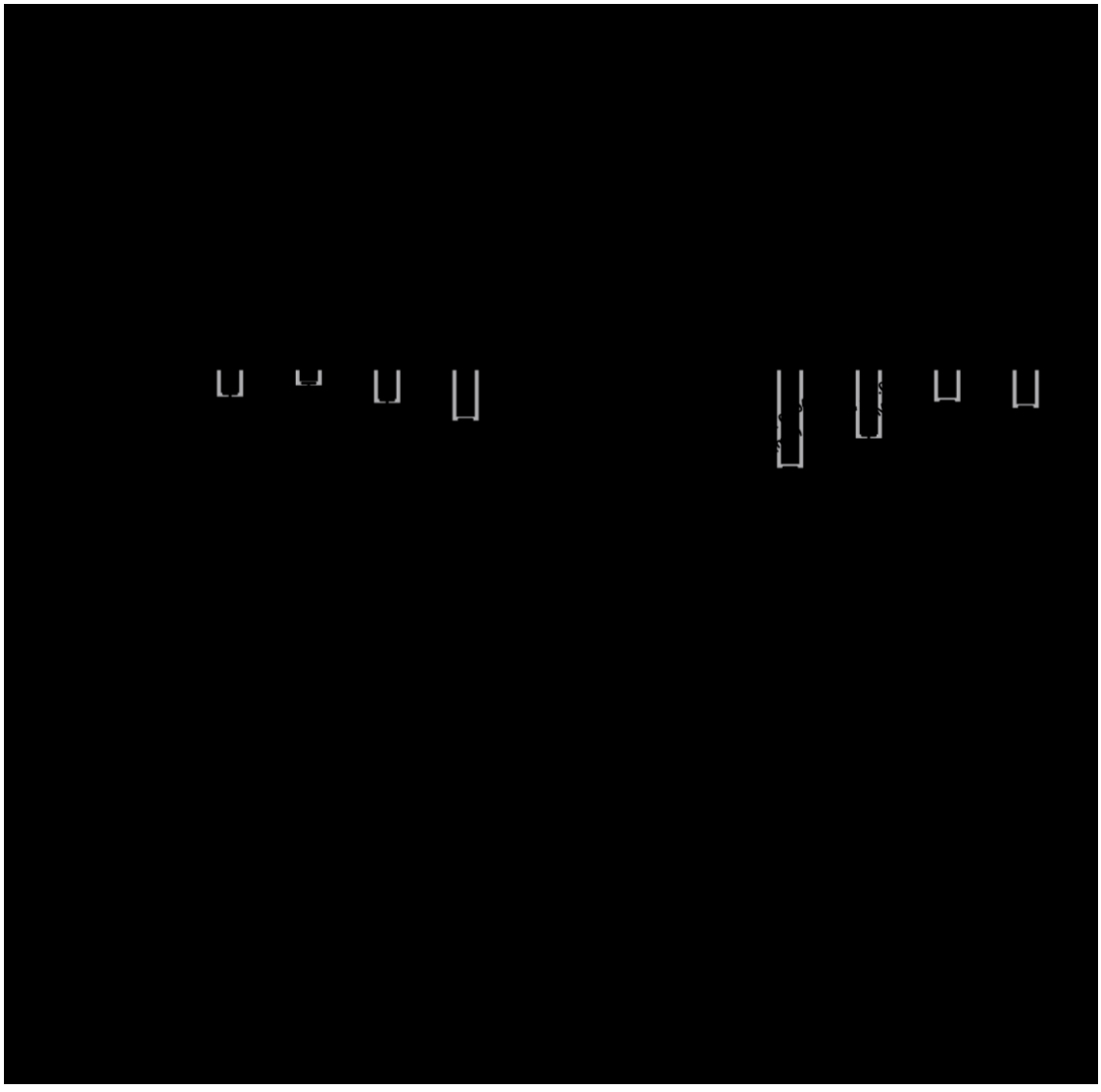

Figure 5. Quantitative analysis of condensed phase components, for LLPS induced by mixing **1** with 0.25 μg/μL RNA in 50 mM Tris, pH 7.5, based on ^{19}F NMR. (**a**) Relative distribution of peptide **1** (%) in the condensed phase (upward bars) and in the dilute phase (downward bars) at different total peptide concentrations. The estimated peptide concentration in each phase is indicated next to each bar. (**b**) Relative distribution of RNA (%) in the condensed phase (upward bars) and in the dilute phase (downward bars) at different total peptide concentrations. The estimated RNA concentration (per-nucleotide basis) is indicated next to each bar. (**c**) Estimated ionic group (Arg^+ on peptide and PO_4^- on RNA) concentrations in the condensed phase at various peptide concentrations. (**d**) Charge ratio (left axis: ratio of Arg^+ on peptide to PO_4^- on RNA; right axis: ratio of total peptide charge to PO_4^- on RNA) at different concentrations of peptide **1** in the condensed phase. Data presented as means ± SD (n = 4). Condensed phase volume at each peptide concentration was measured via ^{19}F NMR as described in the text.

We used the ^{19}F NMR-based quantification method to examine the effect on condensed phase composition of varying the concentration of peptide **1** when RNA was held constant at 0.25 μg/μL in 50 mM Tris, pH 7.5. As shown in Figure **5a**, peptide concentration in the condensed phase increased steadily as the total peptide concentration was increased from 0.05 to 0.2 mM, but this trend diminished between 0.2 and 0.4 mM. The percentage of peptide **1** in the condensed phase was reasonably consistent (75-85%) as the total peptide concentration was varied, but a small decline was evident at the highest concentration. The condensed phase volume did not change significantly across this peptide concentration range (Figure **S10b**). The proportion of RNA in the condensed phase rose steadily between 0.05 and 0.2 mM peptide **1** and leveled off between 0.2 and 0.4 mM of **1** (Figure **5b**). At 0.2 mM **1**, the polycation:polyanion charge ratio (peptide:RNA) in the condensed phase should be ~1:1, if we assume that all basic and acidic side chains groups on the peptide (8 Arg and 3 Glu) are ionized. The predicted polycation:polyanion ratio increased to ~2:1 at 0.4 mM **1**. Trends in predicted concentrations of charged groups from polyions (Figure 5c) and polyion charge ratios (Figure 5d) suggest that the condensed phase can attract an excess of the polycationic peptide, on a charge basis, relative to polyanionic RNA. Such "overcharging" within complex coacervates has been explained based on the favorable entropy associated with counterion release and a favorable combinatorial entropy arising from polycation-polyanion association modes.[41,42]

Peptide concentrations in RNA-rich phases containing two peptides were assessed with the ^{19}F NMR-based method (Figure **6**). Each sample contained 0.25 μg/μL RNA and 0.1 mM **1** (containing 20 mol % **Fl-1**) to ensure LLPS. Samples varied in the identity of the second peptide, also at 0.1 mM. The second peptide contained 20 mol % of the TMR-labeled derivative. This proportion of labeled peptide was necessary to ensure adequate sensitivity in optical measurements of concentration. Control studies showed that varying the proportion of fluorescently labeled peptide did not affect our conclusions (Figure **S11a**). When the second peptide sample was Arg-rich **1** or *ent*-**1**, after 30 minutes incubation, we detected ~90-fold enrichment (based on TMR) in the condensed phase relative to the total peptide concentration. This observation suggests that the concentration of *ent*-**1** in the condensed phase was ~ 9 mM (Figure **6b**). Citrulline-containing peptide **5** was not significantly enriched in droplets (Figure **6b**).

Although neither Lys-rich **2** or ADMA-rich **4** could support formation of a condensed phase with RNA under these conditions (Figure **3**), each of these peptides showed ~70-fold enrichment in the condensed phase formed by **1**+RNA (i.e., the concentration of **2** or **4** within droplets was ~7 mM) (Figure **6b**). These results are consistent with the qualitative microscopy findings discussed above (Figure **4**) and strengthen the conclusion that the ability to support *formation* of an RNA-rich condensed phase and the ability to be *recruited* to and concentrated in such a phase are distinct properties. Our data show that these properties can vary among peptides that differ in the nature of their cationic side chains but have the same net charge and distribution of charged groups.

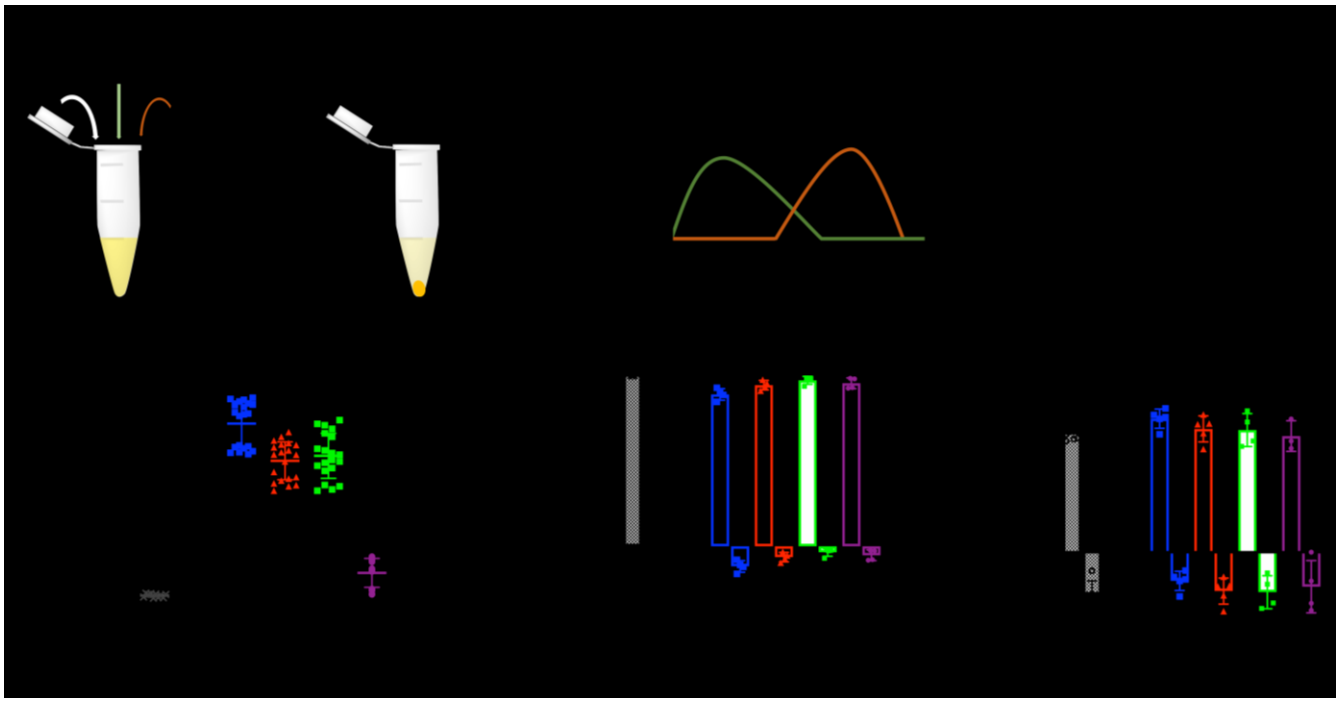

Figure 6. (**a**) Sample preparation for the two-peptide system concentration measurements. 0.1 mM **1** (with 20 mol% **Fl-1**) and 0.1 mM second peptide (with 20 mol% TMR-labeling) were mixed with 0.25 μg/μL RNA in Tris buffer and incubated at room temperature for 30 minutes. The LLPS solution was then spun down to collect the supernatant. The concentration of each component in the supernatant was determined by UV-spectroscopy, and this information along with the volume of the condensed phase determined by ^{19}F NMR was used to determine the enrichment index. (**b**) Estimated enrichment index for the TMR-labeled peptide in the two-peptide experiments. The enrichment index is the ratio of the concentration of the peptide in the condensed phase to the total concentration of that peptide in the sample. Estimated peptide concentrations in the condensed phase are shown on the right vertical axis. Tetramethylrhodamine (TMR) at 0.02 mM

was used as a non-peptide control. (**c**) Displacement of the original peptide **1** by the second peptide, as judged based on Fl fluorescence. Positive scale represents % of **1** remaining in the condensed phase; negative axis represents % of **1** displaced into the dilute phase. (**d**) Distribution of RNA (%) in condensed phase (positive scale) vs. free RNA (%) in dilute phase (negative scale) when different peptides are added. Results shown here are averaged over five fluorine-containing reference compounds. Data presented as means ± SD (n ⩾ 4). P values (P > 0.1234 (ns), P < 0.0001 (****)) were calculated by one way ANOVA.

Previous studies with poly-Arg and poly-Lys showed that one polymer could displace the other from complex coacervates under some conditions.[19] We therefore asked whether the "scaffold" peptide **1** (with 20 mol% **Fl-1**) was displaced from the condensed phase by the second peptide under the conditions we employed. Upon the addition of 0.1 mM **1** or *ent*-**1** to a preformed condensed phase, only a small portion (~10%) of **1** was displaced, as judged by the Fl signal (Figure **6c**). The displacement of **1** by 0.1 mM Lys-rich **2**, ADMA-rich **4** or Cit-rich **5** was insignificant. None of the added peptides caused a significant change in the proportion of RNA in the condensed phase (Figure **6d**).

Dynamics of Condensed Phase Droplets: Distinct Entry Modes. As a complement to the studies described above, in which both peptide samples were simultaneously mixed with the RNA component (Figure S12a), we conducted experiments in which a phase-separated sample was generated by mixing 0.25 μg/μL RNA with 0.1 mM **1** (4 mol% Fl label), and the second peptide (4 mol% TMR label) was added after 2 hours (Figure S12b). Time-lapse microscopy suggested different mechanisms for entry of the second peptide into preformed droplets as a function of side chain. For Lys-rich **2** or ADMA-rich **4**, which do not independently support LLPS with RNA under these conditions, TMR fluorescence entered preformed droplets uniformly around the periphery and moved to the droplet center (Figure **7a**). This process appeared to be complete across the sample within 90 seconds.

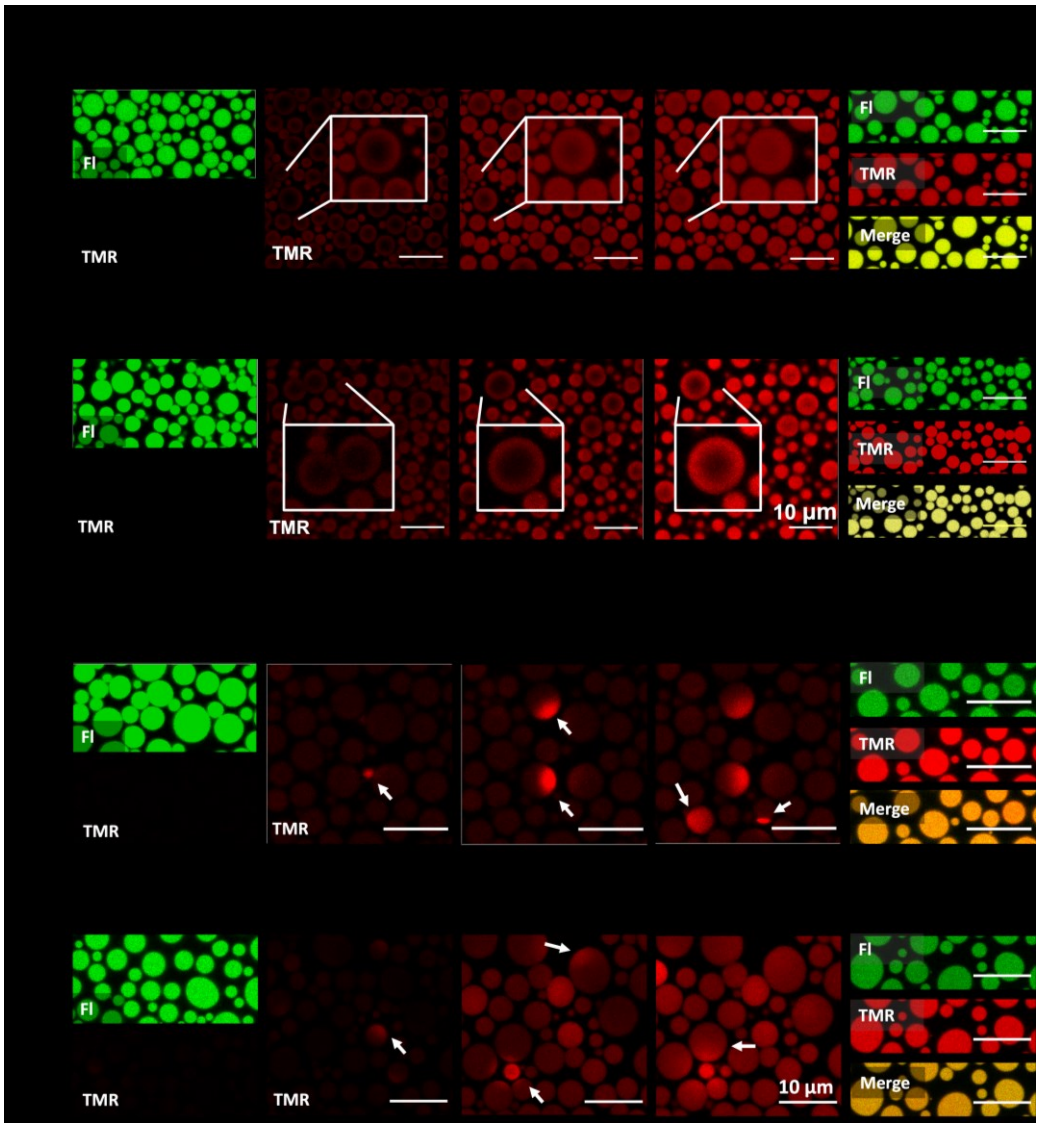

Figure 7. Time-lapse images of peptide recruitment to condensed phase droplets. (**a**) Peptides that did not support LLPS (**2** and **4**) passively diffused into the pre-formed droplets. (**b**) Peptides that supported LLPS (**1** and *ent*-**1**) entered the pre-formed droplets through a "patch". Scale bar = 10 μm.

In contrast, for Arg-rich **1** or *ent*-**1**, TMR fluorescence first appeared in one small region of the droplet edge and then migrated across the entire droplet (Figure **7b**). Some videos showed the sudden appearance of a droplet that displayed high and uniform TMR fluorescence (i.e., fluorescence detected in only the TMR channel) (Video S1). In these cases, subsequent micrographs suggested that TMR-labeled peptide from such droplets rapidly moved to the nearest edges of neighboring droplets, which initially manifested fluorescence in only the fluorescein channel. These images suggest that new droplets may have formed from the added peptide and residual RNA in the dilute phase (Figure **5b** and **6d**), with subsequent exchange of Fl- and TMR-labeled peptides between neighboring droplets. We could not discern whether newly formed TMR-rich droplets were associated with all cases of entry into preformed droplets. These observations raise the possibility that different proteins may be recruited to RNA-rich membraneless organelles via distinct mechanisms depending on the nature of their composition and/or their degree of post-translational modification. Such mechanistic distinctions might be correlated with different consequences in terms of cellular physiology

DISCUSSION

The studies reported here were motivated by the widespread occurrence of liquid-liquid phase separation in cells and by enduring uncertainties about the physicochemical factors that control such phenomena and the functional roles of phase separation in biology.[1-23, 25] We identified a system in which phase separation can be induced by combining an Arg-rich synthetic peptide derived from the protein FUS and heterogeneous RNA. This form of LLPS appears to be mediated by interactions of small moieties, such as individual side chains, that are dispersed along the flexible peptide backbone. Our system allowed us to probe the role of amino acid side chain identity in LLPS arising from polycation-polyanion interaction.

Our results show that Coulombic complementarity is necessary for peptide-RNA LLPS, as would be expected, but that Coulombic attraction is not sufficient for phase separation in this system. The identity of the cationic group is a critical determinant. Thus, replacing Arg residues (guanidinium groups) with either Lys or ADMA residues (ammonium or asymmetric dimethylguanidinium groups) prevents phase separation with RNA under our conditions. These observations are correlated with results reported for FUS protein *self-association*: Arg-to-Lys mutations in the FUS C-terminal domain diminish LLPS propensity, as does post-translational modification of Arg residues to ADMA.[12,25] However, the mechanistic origins of these effects are unclear. For example, it has been proposed that diminished phase separation observed upon Arg-to-ADMA modification results from diminished cation-π attraction between dimethylguanidinium and aromatic groups in the protein relative to cation-π attraction between guanidinium and aromatic groups.[25] This hypothesis seems to be inconsistent with elegant model studies showing that the ADMA side chain forms more favorable cation-π interactions with a Trp side chain than does the unmodified Arg side chain.[43]

The trend we observe among peptides containing **1**, **3** and **4** (Figure **3**), which indicates decreasing LLPS propensity as the side chain is varied from Arg to MMA to ADMA, raises the possibility that the hydrogen bonding properties of the peptide side chains may be critical for phase-separation mediated by Arg-rich peptides or proteins and RNA. Guanidinium and phosphate groups can associate via monodentate and bidentate hydrogen bonding motifs (Figure **8a,b**).[44–46] The Arg side chain offers five possibilities for the monodentate H-bond motif, MMA offers four, and ADMA offers three. For the bidentate H-bond motif, the Arg side chain offers two possibilities, MMA offers one, and the ADMA side chain does not allow this motif (Figure **8c-e**; the position of the Arg side chain δ carbon relative to the methyl group(s) is constrained by the need to avoid a *syn*-pentane-like interaction). Thus, post-translational arginine methylation reduces H-bond options with phosphate groups on RNA, a trend that could explain the variations we observe in the abilities of peptides **1**, **3** and **4** to support LLPS with RNA. The bidentate H-bond motif might be particularly important to support LLPS in our system; it is not clear that a bidentate H-bond motif is favorable for an ammonium group.

The studies reported here demonstrate a difference between the network of noncovalent forces between a cationic polypeptide and RNA that is required to support *formation* of a condensed phase and the network required for *recruitment* to a preexisting condensed phase. Recruitment, at least in our system, may depend only on Coulombic attraction between polyions, presumably with concomitant counterion release, while formation of the condensed phase seems to require additional noncovalent attraction, possibly including a specific bidentate H-bonding motif (Figure **8b**). The distinction between *formation* of and *recruitment* to membraneless organelles and other intracellular assemblies may prove important for elucidating the biological functions of these assemblies.

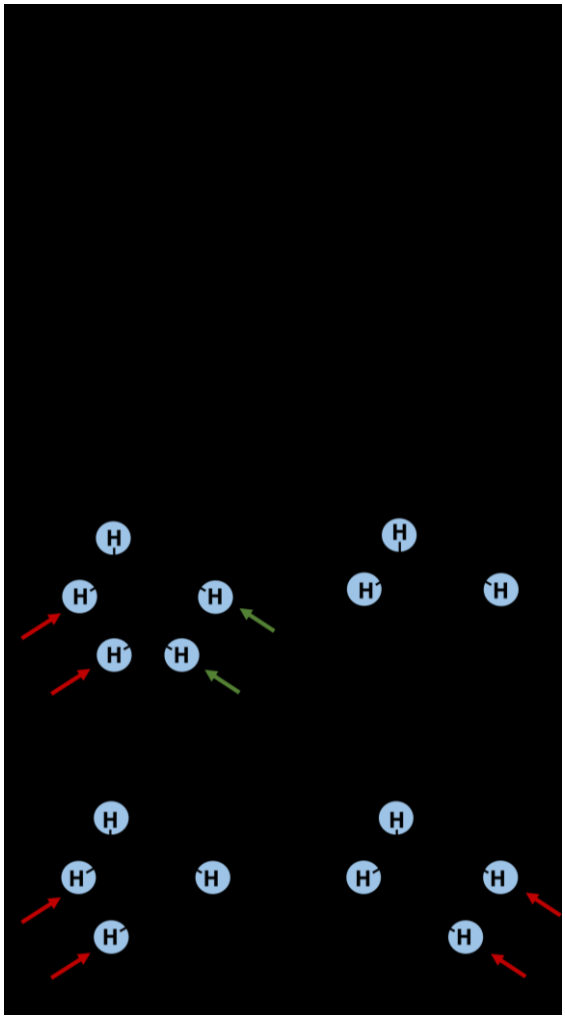

Figure 8. Hydrogen bonding patterns between arginine peptide and RNA. (**a**) Monodentate H-bond motif between arginine side chain and phosphate group on RNA. (**b**) Bidentate H-bonding motif. (**c**) Five monodentate (blue circles) and two bidentate (arrows) H-bonding sites possible for arginine. (**d**) Three monodentate (blue circles) and zero bidentate H-bonding sites possible for asymmetric dimethylated arginine. (**e**) Four monodentate (blue circles) and one bidentate (arrows) H-bonding sites possible for monomethylated arginine.

An important feature of this study is the new strategy we have developed for measuring concentrations of molecules within condensed phases. The ^{19}F NMR-based method allowed us to determine that cationic peptides incapable of supporting LLPS in combination with RNA could nevertheless achieve relatively high concentrations (~7 mM) within a condensed phase scaffolded by an Arg-rich peptide and RNA, approaching the concentration of the Arg-rich peptide (~9 mM). The difficulty of quantifying component concentrations in condensed phases is widely recognized, as evidenced by the many studies that do not provide such information. For *in vitro* studies, the molecules required to induce LLPS are often not readily available in large quantities (e.g., the synthetic peptides we employed, or an expressed protein). At typical experimental scales, the condensed phase generated in such systems has a volume of $\leq$ 5 μL, which is difficult to measure directly with accuracy. The use of non-interactive fluorine-containing compounds, which are available in diverse forms, enables reliable and convenient concentration determinations for many parallel condensed phase samples, which is necessary for comparative studies of the type reported here.

Although many questions remain open regarding mechanisms of LLPS in cells and the functional outcomes of such processes, it is clear that this unique mode of compartmentalization has been harnessed by evolution.[2,20,31] Insights gained from the rapidly expanding appreciation of LLPS in biology are inspiring the exploration of new applications of LLPS in non-biological contexts.[13,16,19,39] Elucidation of the principles that control the formation of condensed liquid phases and the transit of molecules between contiguous condensed and dilute phases is necessary for to understand LLPS roles in biology and to harness the potential of LLPS-based engineering in chemical systems. The insights and tools described here contribute to this long-term goal.

ASSOCIATED CONTENT

Supporting Information

The Supporting Information is available free of charge on the ACS Publications website.

Materials (Section I), method descriptions (Section II), additional figures and tables (Section III), ^{19}F-NMR data (Section IV) and characterization data for all synthesized peptides (Section V) (PDF)

AUTHOR INFORMATION

Corresponding Authors

Samuel H. Gellman − Department of Chemistry, University of Wisconsin, Madison, Wisconsin 53706, United States; orcid.org/0000-0001-5617-0058; Email: gellman@ chem.wisc.edu

Nicholas L. Abbott − Robert F. Smith School of Chemical and Biomolecular Engineering, Cornell University, New York 14853, United States; orcid.org/0000-0002-9653-0326; Email: nla34@cornell.edu

Authors

Jiani Niu − Department of Chemistry, University of Wisconsin, Madison, Wisconsin 53706, United States; orcid.org/0000-0002-5090-5516; Email: jniu23@ chem.wisc.edu

Cindy Qiu − Robert F. Smith School of Chemical and Biomolecular Engineering, Cornell University, New York 14853, United States; orcid.org/0000-0001-6131-3586; Email: xq75@cornell.edu

Notes

The authors declare no competing interests.

ACKNOWLEDGMENT

This work was supported in part by a grant from NIGMS (R01 GM061238) and NSF (DMR-2003807).

REFERENCES

(1) Nott, T. J.; Petsalaki, E.; Farber, P.; Jervis, D.; Fussner, E.; Plochowietz, A.; Craggs, T. D.; Bazett-Jones, D. P.; Pawson, T.; Forman-Kay, J. D.; et al. Phase Transition of a Disordered Nuage Protein Generates Environmentally Responsive Membraneless Organelles. *Mol. Cell* **2015**, *57* (5), 936–947.

https://doi.org/10.1016/j.molcel.2015.01.013.

(2) Shin, Y.; Brangwynne, C. P. Liquid Phase Condensation in Cell Physiology and Disease. *Science (80-.).* **2017**, *357* (6357). https://doi.org/10.1126/science.aaf4382.

(3) Lee, K. H.; Zhang, P.; Kim, H. J.; Mitrea, D. M.; Sarkar, M.; Freibaum, B. D.; Cika, J.; Coughlin, M.; Messing, J.; Molliex, A.; et al. C9orf72 Dipeptide Repeats Impair the Assembly, Dynamics, and Function of Membrane-Less Organelles. *Cell* **2016**, *167* (3), 774-788.e17. https://doi.org/10.1016/j.cell.2016.10.002.

(4) Feng, Z.; Jia, B.; Zhang, M. Liquid-Liquid Phase Separation in Biology: Specific Stoichiometric Molecular Interactions vs Promiscuous Interactions Mediated by Disordered Sequences. *Biochemistry*. 2021, pp 2397–2406. https://doi.org/10.1021/acs.biochem.1c00376.

(5) Courchaine, E. M.; Barentine, A. E. S.; Straube, K.; Lee, D.-R.; Bewersdorf, J.; Neugebauer, K. M. DMA-Tudor Interaction Modules Control the Specificity of in Vivo Condensates. *Cell* **2021**, *184* (14), 3612-3625.e17. https://doi.org/10.1016/j.cell.2021.05.008.

(6) White, M. R.; Mitrea, D. M.; Zhang, P.; Stanley, C. B.; Cassidy, D. E.; Nourse, A.; Phillips, A. H.; Tolbert, M.; Taylor, J. P.; Kriwacki, R. W. C9orf72 Poly(PR) Dipeptide Repeats Disturb Biomolecular Phase Separation and Disrupt Nucleolar Function. *Mol. Cell* **2019**, *74* (4), 713-728.e6. https://doi.org/10.1016/j.molcel.2019.03.019.

(7) Mitrea, D. M.; Cika, J. A.; Guy, C. S.; Ban, D.; Banerjee, P. R.; Stanley, C. B.; Nourse, A.; Deniz, A. A.; Kriwacki, R. W. Nucleophosmin Integrates within the Nucleolus via Multi-Modal Interactions with Proteins Displaying R-Rich Linear Motifs and RRNA. *Elife* **2016**, *5*, 1–33. https://doi.org/10.7554/elife.13571.

(8) Iwata, T.; Hirose, H.; Sakamoto, K.; Hirai, Y.; Arafiles, J. V. V.; Akishiba, M.; Imanishi, M.; Futaki, S. Liquid Droplet Formation and Facile Cytosolic Translocation of IgG in the Presence of Attenuated Cationic Amphiphilic Lytic Peptides. *Angew. Chemie Int. Ed.* **2021**. https://doi.org/10.1002/anie.202105527.

(9) Mitrea, D. M.; Cika, J. A.; Stanley, C. B.; Nourse, A.; Onuchic, P. L.; Banerjee, P. R.; Phillips, A. H.; Park, C. G.; Deniz, A. A.; Kriwacki, R. W. Self-Interaction of NPM1 Modulates Multiple Mechanisms of Liquid-Liquid Phase Separation. *Nat. Commun.* **2018**, *9* (1), 1–13. https://doi.org/10.1038/s41467-018-03255-3.

(10) Ghosh, A.; Mazarakos, K.; Zhou, H. X. Three Archetypical Classes of Macromolecular Regulators of Protein Liquid-Liquid Phase Separation. *Proc. Natl. Acad. Sci. U. S. A.* **2019**, *116* (39), 19474–19483. https://doi.org/10.1073/pnas.1907849116.

(11) Carter, G. C.; Hsiung, C. H.; Simpson, L.; Yang, H.; Zhang, X. N-Terminal Domain of TDP43 Enhances Liquid-Liquid Phase Separation of Globular Proteins. *J. Mol. Biol.* **2021**, *433* (10), 166948. https://doi.org/10.1016/j.jmb.2021.166948.

(12) Wang, J.; Choi, J. M.; Holehouse, A. S.; Lee, H. O.; Zhang, X.; Jahnel, M.; Maharana, S.; Lemaitre, R.; Pozniakovsky, A.; Drechsel, D.; et al. A Molecular Grammar Governing the Driving Forces for Phase Separation of Prion-like RNA Binding Proteins. *Cell* **2018**, *174* (3), 688-699.e16. https://doi.org/10.1016/j.cell.2018.06.006.

(13) Aumiller, W. M.; Pir Cakmak, F.; Davis, B. W.; Keating, C. D. RNA-Based Coacervates as a Model for Membraneless Organelles: Formation, Properties, and Interfacial Liposome Assembly. *Langmuir* **2016**, *32* (39), 10042–10053. https://doi.org/10.1021/acs.langmuir.6b02499.

(14) Cakmak, F. P.; Choi, S.; Meyer, M. C. O.; Bevilacqua, P. C.; Keating, C. D. Prebiotically-Relevant Low Polyion Multivalency Can Improve Functionality of Membraneless Compartments. *Nat. Commun.* **2020**, *11* (1), 1–11. https://doi.org/10.1038/s41467-020-19775-w.

(15) Harami, G. M.; Kovács, Z. J.; Pancsa, R.; Pálinkás, J.; Baráth, V.; Tárnok, K.; Málnási-Csizmadia, A.; Kovács, M. Phase Separation by SsDNA Binding Protein Controlled via Protein-Protein and Protein-DNA Interactions. *Proc. Natl. Acad. Sci. U. S. A.* **2020**, *117* (42), 26206–26217. https://doi.org/10.1073/pnas.2000761117.

(16) Lytle, T. K.; Chang, L. W.; Markiewicz, N.; Perry, S. L.; Sing, C. E. Designing Electrostatic Interactions via Polyelectrolyte Monomer Sequence. *ACS Cent. Sci.* **2019**, *5* (4), 709–718. https://doi.org/10.1021/acscentsci.9b00087.

(17) Perry, S. L.; Leon, L.; Hoffmann, K. Q.; Kade, M. J.; Priftis, D.; Black, K. A.; Wong, D.; Klein, R. A.; Pierce, C. F.; Margossian, K. O.; et al. Chirality-Selected Phase Behaviour in Ionic Polypeptide Complexes. *Nat. Commun.* **2015**, *6*. https://doi.org/10.1038/ncomms7052.

(18) Boeynaems, S.; Holehouse, A. S.; Weinhardt, V.; Kovacs, D.; Van Lindt, J.; Larabell, C.; Bosch, L. Van Den; Das, R.; Tompa, P. S.; Pappu, R. V.; et al. Spontaneous Driving Forces Give Rise to Protein−RNA Condensates with Coexisting Phases and Complex Material Properties. *Proc. Natl. Acad. Sci. U. S. A.* **2019**, *116* (16), 7889–7898. https://doi.org/10.1073/pnas.1821038116.

(19) Fisher, R. S.; Elbaum-Garfinkle, S. Tunable Multiphase Dynamics of Arginine and Lysine Liquid Condensates. *Nat. Commun.* **2020**, *11* (1). https://doi.org/10.1038/s41467-020-18224-y.

(20) Hyman, A. A.; Weber, C. A.; Jülicher, F. Liquid-Liquid Phase Separation in Biology. *Annu. Rev. Cell Dev. Biol.* **2014**, *30*, 39–58. https://doi.org/10.1146/annurev-cellbio-100913-013325.

(21) Boeynaems, S.; Alberti, S.; Fawzi, N. L.; Mittag, T.; Polymenidou, M.; Rousseau, F.; Schymkowitz, J.; Shorter, J.; Wolozin, B.; Van Den Bosch, L.; et al. Protein Phase Separation: A New Phase in Cell Biology. *Trends in Cell Biology*. 2018, pp 420–435. https://doi.org/10.1016/j.tcb.2018.02.004.

(22) Ditlev, J. A.; Case, L. B.; Rosen, M. K. Who's In and Who's Out—Compositional Control of Biomolecular Condensates. *J. Mol. Biol.* **2018**, *430* (23), 4666–4684. https://doi.org/10.1016/j.jmb.2018.08.003.

(23) Su, Q.; Mehta, S.; Zhang, J. Liquid-Liquid Phase Separation: Orchestrating Cell Signaling through Time and Space. *Molecular Cell*. 2021, pp 4137–4146. https://doi.org/10.1016/j.molcel.2021.09.010.

(24) Murray, D. T.; Kato, M.; Lin, Y.; Thurber, K. R.; Hung, I.; McKnight, S. L.; Tycko, R. Structure of FUS Protein Fibrils and Its Relevance to Self-Assembly and Phase Separation of Low-Complexity Domains. *Cell* **2017**, *171* (3), 615-627.e16. https://doi.org/10.1016/j.cell.2017.08.048.

(25) Qamar, S.; Wang, G. Z.; Randle, S. J.; Ruggeri, F. S.; Varela, J. A.; Lin, J. Q.; Phillips, E. C.; Miyashita, A.; Williams, D.; Ströhl, F.; et al. FUS Phase Separation Is Modulated by a Molecular Chaperone and Methylation of Arginine Cation-π Interactions. *Cell* **2018**, *173* (3), 720-734.e15. https://doi.org/10.1016/j.cell.2018.03.056.

(26) Luo, F.; Gui, X.; Zhou, H.; Gu, J.; Li, Y.; Liu, X.; Zhao, M.; Li, D.; Li, X.; Liu, C. Atomic Structures of FUS LC Domain Segments Reveal Bases for Reversible Amyloid Fibril Formation. *Nat. Struct. Mol. Biol.* **2018**, *25* (4), 341–346. https://doi.org/10.1038/s41594-018-0050-8.

(27) Patel, A.; Lee, H. O.; Jawerth, L.; Maharana, S.; Jahnel, M.; Hein, M. Y.; Stoynov, S.; Mahamid, J.; Saha, S.; Franzmann, T. M.; et al. A Liquid-to-Solid Phase Transition of the ALS Protein FUS Accelerated by Disease Mutation. *Cell* **2015**, *162* (5), 1066–1077. https://doi.org/10.1016/j.cell.2015.07.047.

(28) Wiedner, H. J.; Giudice, J. It's Not Just a Phase: Function and Characteristics of RNA-Binding Proteins in Phase Separation. *Nat. Struct. Mol. Biol.* **2021**, *28* (6), 465–473. https://doi.org/10.1038/s41594-021-00601-w.

(29) Vasilyev, N.; Polonskaia, A.; Darnell, J. C.; Darnell, R. B.; Patel, D. J.; Serganov, A. Crystal Structure Reveals Specific Recognition of a G-Quadruplex RNA by a β-Turn in the RGG Motif of FMRP. *Proc. Natl. Acad. Sci. U. S. A.* **2015**, *112* (39), E5391–E5400. https://doi.org/10.1073/pnas.1515737112.

(30) Ukmar-Godec, T.; Hutten, S.; Grieshop, M. P.; Rezaei-Ghaleh, N.; Cima-Omori, M. S.; Biernat, J.; Mandelkow, E.; Söding, J.; Dormann, D.; Zweckstetter, M. Lysine/RNA-Interactions Drive and Regulate Biomolecular Condensation. *Nat. Commun.* **2019**, *10* (1). https://doi.org/10.1038/s41467-019-10792-y.

(31) Brangwynne, C. P.; Tompa, P.; Pappu, R. V. Polymer Physics of Intracellular Phase Transitions. *Nat. Phys.* **2015**, *11* (11), 899–904. https://doi.org/10.1038/nphys3532.

(32) Alshareedah, I.; Moosa, M. M.; Raju, M.; Potoyan, D. A.; Banerjee, P. R. Phase Transition of RNA−protein Complexes into Ordered Hollow Condensates. *Proc. Natl. Acad. Sci. U. S. A.*

2020, *117* (27), 15650–15658. https://doi.org/10.1073/pnas.1922365117.

(33) Manning, G. S. Counterion Binding in Polyelectrolyte Theory. *Acc. Chem. Res.* **1979**, *12* (12), 443–449. https://doi.org/10.1021/ar50144a004.

(34) Anderson, Charles F; Record, Jr, M. T. Salt-Nucleic Acid Interactions. *Annu. Rev. Phys. Chem.* **1995**, *46* (1), 657–700.

(35) Lipfert, J.; Doniach, S.; Das, R.; Herschlag, D. Understanding Nucleic Acid-Ion Interactions. *Annu. Rev. Biochem.* **2014**, *83*, 813–841. https://doi.org/10.1146/annurev-biochem-060409-092720.

(36) Alshareedah, I.; Kaur, T.; Ngo, J.; Seppala, H.; Kounatse, L. A. D.; Wang, W.; Moosa, M. M.; Banerjee, P. R. Interplay between Short-Range Attraction and Long-Range Repulsion Controls Reentrant Liquid Condensation of Ribonucleoprotein-RNA Complexes. *J. Am. Chem. Soc.* **2019**, *141* (37), 14593–14602. https://doi.org/10.1021/jacs.9b03689.

(37) Lorton, B. M.; Shechter, D. Cellular Consequences of Arginine Methylation. *Cell. Mol. Life Sci.* **2019**, *76* (15), 2933–2956. https://doi.org/10.1007/s00018-019-03140-2.

(38) Criscitiello, M. F.; Kraev, I.; Lange, S. Deiminated Proteins in Extracellular Vesicles and Serum of Llama (Lama Glama)—Novel Insights into Camelid Immunity. *Mol. Immunol.* **2020**, *117*, 37–53. https://doi.org/10.1016/j.molimm.2019.10.017.

(39) Abbas, M.; Lipiński, W. P.; Nakashima, K. K.; Huck, W. T. S.; Spruijt, E. A Short Peptide Synthon for Liquid–Liquid Phase Separation. *Nat. Chem.* **2021**, *13* (11), 1046–1054. https://doi.org/10.1038/s41557-021-00788-x.

(40) Aumiller, W. M.; Keating, C. D. Phosphorylation-Mediated RNA/Peptide Complex Coacervation as a Model for Intracellular Liquid Organelles. *Nat. Chem.* **2016**, *8* (2), 129–137. https://doi.org/10.1038/nchem.2414.

(41) Ghasemi, M.; Friedowitz, S.; Larson, R. G. Overcharging of Polyelectrolyte Complexes: An Entropic Phenomenon. *Soft Matter* **2020**, *16* (47), 10640–10656. https://doi.org/10.1039/d0sm01466d.

(42) Lytle, T. K.; Sing, C. E. Transfer Matrix Theory of Polymer Complex Coacervation. *Soft Matter* **2017**, *13* (39), 7001–7012. https://doi.org/10.1039/c7sm01080j.

(43) Hughes, R. M.; Waters, M. L. Arginine Methylation in a β-Hairpin Peptide: Implications for Arg-π Interactions, ΔCp°, and the Cold Denatured State. *J. Am. Chem. Soc.* **2006**, *128* (39), 12735–12742. https://doi.org/10.1021/ja061656g.

(44) Hirsch, A. K. H.; Fischer, F. R.; Diederich, F. Phosphate Recognition in Structural Biology. *Angew. Chemie - Int. Ed.* **2007**, *46* (3), 338–352. https://doi.org/10.1002/anie.200603420.

(45) Frigyes, D.; Alber, F.; Pongor, S.; Carloni, P. Arginine-Phosphate Salt Bridges in Protein-DNA Complexes: A Car-Parrinello Study. *J. Mol. Struct. THEOCHEM* **2001**, *574* (1–3), 39–45. https://doi.org/10.1016/S0166-1280(01)00368-2.

(46) Kneeland, D. M.; Ariga, K.; Lynch, V. M.; Huang, C. Y.; Anslyn, E. V. Bis(Alkylguanidinium) Receptors for Phosphodiesters: Effect of Counterions, Solvent Mixtures, and Cavity Flexibility on Complexation. *J. Am. Chem. Soc.* **1993**, *115* (22), 10042–10055. https://doi.org/10.1021/ja00075a021.